



# Lawrence Berkeley Laboratory

UNIVERSITY OF CALIFORNIA

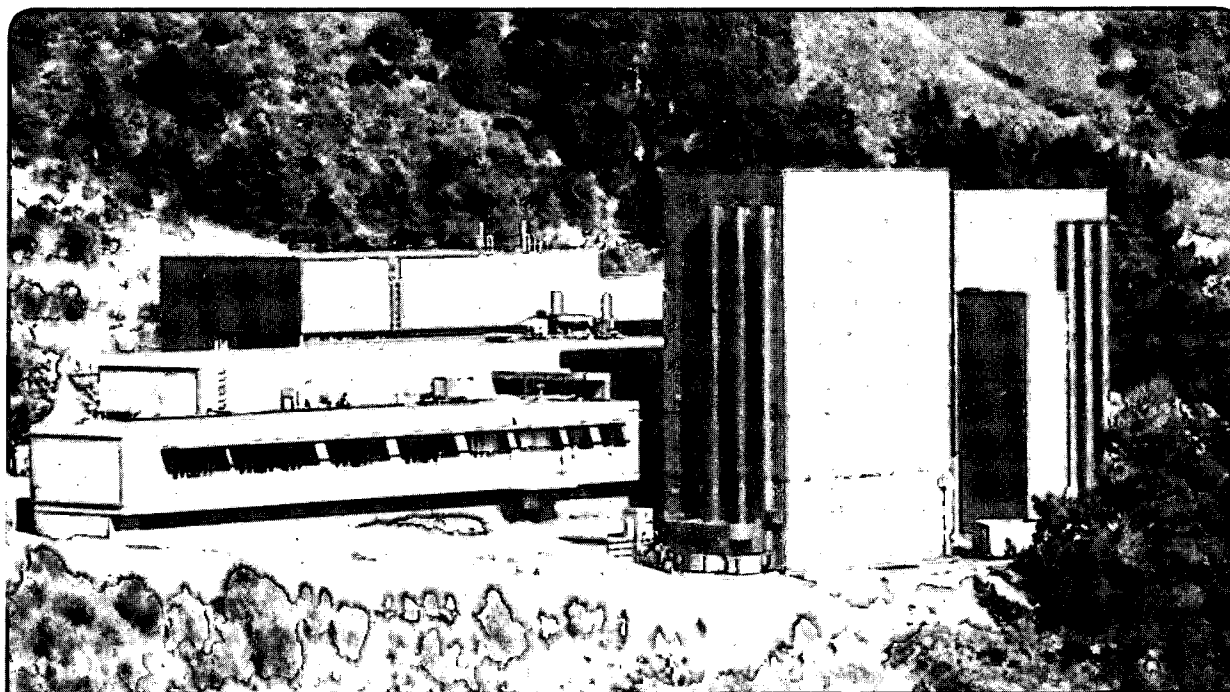
## Materials Sciences Division National Center for Electron Microscopy

Presented at the 6th International Conference on Intergranular and Interphase Boundaries in Materials, Thessaloniki, Greece, June 21-26, 1992, and to be published in the Proceedings

### Grain Boundaries in Mazed Multicrystal Microstructures of Al

U. Dahmen and N. Thangaraj

June 1992



Prepared for the U.S. Department of Energy under Contract Number DE-AC03-76SF00098

LOAN COPY  
Circulates  
for 4 weeks

Bldg. 50 Library.  
Copy 2

LBL-33469

### DISCLAIMER

This document was prepared as an account of work sponsored by the United States Government. Neither the United States Government nor any agency thereof, nor The Regents of the University of California, nor any of their employees, makes any warranty, express or implied, or assumes any legal liability or responsibility for the accuracy, completeness, or usefulness of any information, apparatus, product, or process disclosed, or represents that its use would not infringe privately owned rights. Reference herein to any specific commercial product, process, or service by its trade name, trademark, manufacturer, or otherwise, does not necessarily constitute or imply its endorsement, recommendation, or favoring by the United States Government or any agency thereof, or The Regents of the University of California. The views and opinions of authors expressed herein do not necessarily state or reflect those of the United States Government or any agency thereof or The Regents of the University of California and shall not be used for advertising or product endorsement purposes.

Lawrence Berkeley Laboratory is an equal opportunity employer.



Printed on recycled paper

## **DISCLAIMER**

This document was prepared as an account of work sponsored by the United States Government. While this document is believed to contain correct information, neither the United States Government nor any agency thereof, nor the Regents of the University of California, nor any of their employees, makes any warranty, express or implied, or assumes any legal responsibility for the accuracy, completeness, or usefulness of any information, apparatus, product, or process disclosed, or represents that its use would not infringe privately owned rights. Reference herein to any specific commercial product, process, or service by its trade name, trademark, manufacturer, or otherwise, does not necessarily constitute or imply its endorsement, recommendation, or favoring by the United States Government or any agency thereof, or the Regents of the University of California. The views and opinions of authors expressed herein do not necessarily state or reflect those of the United States Government or any agency thereof or the Regents of the University of California.

**Grain Boundaries in Mazed  
Multicrystal Microstructures of Al**

U. Dahmen, and N. Thangaraj

Materials Science Division  
National Center for Electron Microscopy  
Lawrence Berkeley Laboratory  
University of California, Berkeley, CA 94720

Conf. on Intergranular & Interphase Boundaries  
6/21-6/26/92 Thessaloniki, Greece  
Proc. iib(II) (1992) in press.

This work was supported in part by the Director, Office of Energy Research, Office of Basic Energy Sciences, Materials Science Division of the U.S. Department of Energy under Contract No. DE-AC03-76SF00098.

# GRAIN BOUNDARIES IN MAZED MULTICRYSTAL MICROSTRUCTURES OF AL

U. DAHMEN and N. THANGARAJ

National Center for Electron Microscopy, Lawrence Berkeley Laboratory  
University of California, Berkeley, CA. 94720

**KEY WORDS:** Bicrystal, Tricrystal, Al, Heteroepitaxy, Grain Boundaries, Si Substrate, Color Symmetry, Faceting, High Resolution Transmission Electron Microscopy

## ABSTRACT

Thin films of aluminum with mazed bi- and tricrystal microstructures have been produced by exploiting symmetry properties inherent in heteroepitaxial growth. These microstructures are best described as polycrystalline thin films with only two or three allowed grain orientations, rotated  $90^\circ$  or  $30^\circ$  with respect to each other. This work illustrates the unique crystallographic color symmetry and topological properties of mazed bi- and tri-crystal thin films. The faceting and atomic relaxation behavior of these films has been characterized by conventional and high resolution electron microscopy. Mazed bicrystal films have no triple junctions, and mazed tricrystal films exhibit well-controlled junctions where three identical grain boundaries meeting in a triple line. High resolution electron microscopy of significant facets, i.e. boundaries with optimum inclinations illustrates the nature of atomic relaxations in some of these grain boundaries.

## INTRODUCTION

Grain boundary structure and grain morphology in polycrystalline thin films are of great interest, both from a fundamental scientific point of view as well as for thin film applications. The thermal, morphological, mechanical and electrical stability of polycrystalline thin films with varying degrees of texture and morphological complexity is currently under intense investigation. Most deposited films exhibit a texture that is determined by the growth kinetics, such as a  $\langle 111 \rangle$  fiber texture for fcc films in which the  $\{111\}$  face as the slowest-growing surface is parallel to the substrate, without preferred in-plane alignment. In such films, grain boundaries are of the  $\langle 111 \rangle$  tilt type with random tilt angle. However, in-plane alignment can be achieved under certain growth conditions on a single crystal substrate. Such films can be considered an approximation to the more general polycrystalline film microstructures and as such are useful test objects for the study of microstructural behavior of polycrystalline thin films.

It has been shown recently that by using heteroepitaxial thin film growth, films of Al with a 'mazed' multicrystal microstructure can be formed on a single crystal substrate of Si [1,2]. Such microstructures arise naturally if the deposit grows in several symmetry-related orientation variants [3]. Mazed multicrystal films are best visualized as polycrystalline films with only a limited number of allowed grain orientations. This is illustrated schematically in figure 1 which shows a picture of a general polycrystalline grain structure idealized as a honeycomb lattice of hexagonal grains, all with different random orientation. If the same hexagonal tiling is randomly occupied by only two grain orientations, indicated as black and white, then a structure such as that illustrated in figure 1b results. Note that since only two orientations are allowed, the misorientation is fixed for all grain boundaries. However, the inclination of the grain boundaries, i.e. the orientation of the boundary plane may be random. The grains form a convoluted 'mazed' or jig saw puzzle-like morphology which admits all boundary inclinations. During annealing, such a mazed bicrystal structure may coarsen and facet into preferred boundary orientations.

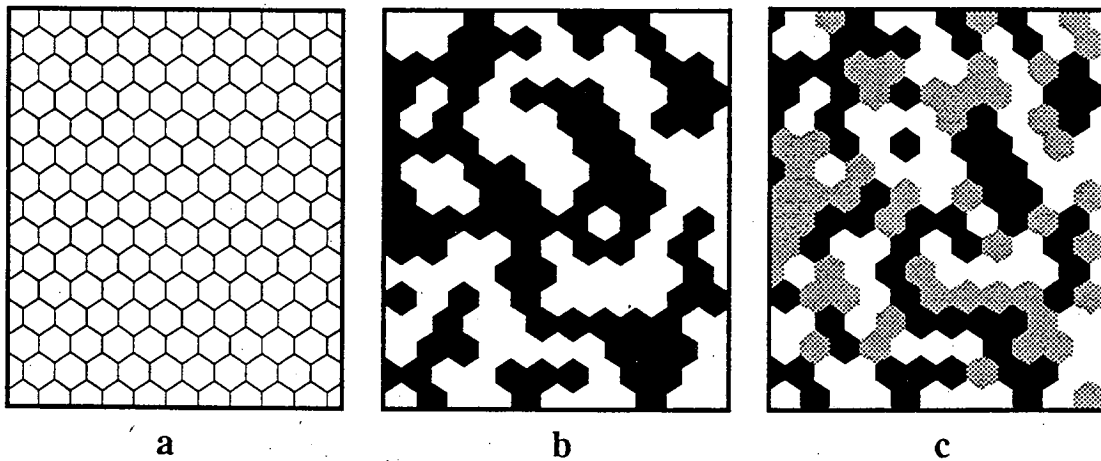


Figure 1: Schematic of general polycrystalline microstructure (a) and its random occupation by only two orientation variants (b) to form a mazed bicrystal microstructure. In (c) the same honeycomb tiling is occupied by three orientation variants shown as three colors. The resulting microstructure is a mazed tricrystal geometry.

Notice that a unique feature of this geometry is the absence of triple junctions [4]. This is different for the mazed tricrystal morphology, illustrated in figure 1c. Here, the hexagonal tiling has been occupied at random by three different orientations, indicated as black, white and gray. The resulting tricrystal geometry displays triple junctions as well as dual facet junctions [5]. However, if the three grains are misoriented by  $120^\circ$  to each other, all grain boundaries will still be of the same misorientation. This results in the unique situation where three identical boundaries can meet in a triple line.

Both microstructures have interesting color symmetries that depend on the crystallographic symmetries of the substrate, the film and their orientation relationship. Other, higher order multicrystal structures could be grown as further approximations to general polycrystalline films. However, the present work will focus on initial experiments on bi- and tricrystal films and a comparison between them.

## EXPERIMENTAL

Al films of thickness 100-300 nm were vacuum deposited from an Al charge of 99.999% purity on single crystal p-type Si (111) and (100) wafers under a base pressure of  $2 \times 10^{-7}$  mbar. The substrates were cleaned by initially oxidizing in a solution of 1:1 by volume hydrogen peroxide and sulfuric acid for about 10 minutes, cleaning with deionized water and finally etching for about 10 min in a solution of 10% HF in deionized water, followed by a water rinse. Prior to deposition, the substrates were heated to various temperatures between room temperature and 450°C by a substrate heater with a Ta base. The texture of as-deposited films was characterized by x-ray diffractometry and the in-plane orientation and the film quality were examined by transmission electron microscopy. X-ray photoelectron spectroscopy and secondary-ion mass spectroscopy were used to probe the interface purity. Plan view TEM samples were prepared by cutting 3mm discs, mechanical dimpling from the substrate side to less than 10  $\mu\text{m}$  and Ar ion thinning to electron transparency. Electron microscopy was performed on 200 kV microscopes, and high resolution images were obtained on the Berkeley ARM 1000 at an operating voltage of 800 kV.

## RESULTS

Under the experimental conditions outlined above and at substrate temperatures of 280°C thin films on (100) Si substrates formed with the following orientation relationship:

$$011_{\text{Al}} \parallel 100_{\text{Si}} \text{ (interface plane)}$$

$$0\bar{1}1_{\text{Al}} \parallel 0\bar{1}1_{\text{Si}}$$

$$100_{\text{Al}} \parallel 011_{\text{Si}}$$

A selected area diffraction pattern showing the  $\langle 001 \rangle$  Si and two superimposed  $\langle 110 \rangle$  Al orientations is seen in fig. 2a. The  $\langle 001 \rangle$  Si pattern is clearly recognizable whereas the Al patterns are obscured by extensive double diffraction. When the Si substrate is removed by backthinning from the Si side, only the two  $\langle 110 \rangle$  orientation variants of Al remain, as shown in fig. 2b. For clarity one of the variants, or grain orientations, has been marked with black dots. The symmetry relations that interchange the black and the white patterns (color symmetry) are the point symmetry elements of the substrate that are not shared by the deposit [6,7]. These color symmetry operations are the 90° rotation and the vertical and horizontal mirrors, whose traces are indicated as white lines. In contrast, the 180° rotation and the diagonal mirrors (also marked) are common to the substrate and the film. The first type of operations exchange the black and white crystal orientations whereas the second type returns each orientation to itself.

The 2-dimensional point group of the bicrystal in this case is the square color symmetry group  $4\text{mm}$ , and its relationship to the rectangular group  $2\text{mm}$  can be described as the following coset decomposition [8] where each of the two cosets may be associated with one of the two colors:

$$4\text{mm} = \{2\text{mm}\} \cup \underline{4^1}\{2\text{mm}\}. \quad (1)$$

Here  $\underline{4^1}$  is a 90° rotation (the underline denotes a color exchange operation),  $\{2\text{mm}\}$  is the group of symmetry elements that map each orientation variant onto itself, and  $\underline{4^1}\{2\text{mm}\}$  is the set of symmetry elements that exchange orientation variants (color exchange operations). This is illustrated in fig. 3 which shows the 2-dimensional point groups and illustrates equ. 1 symbolically. The point group of the bicrystal  $4\text{mm}$  is the union of the point group of the Al film  $2\text{mm}$  and the color exchange set

$4^1\{2mm\}$ . Symmetry elements are denoted by the usual symbols. Color symmetry elements are shown by broken lines or black and white symbols.

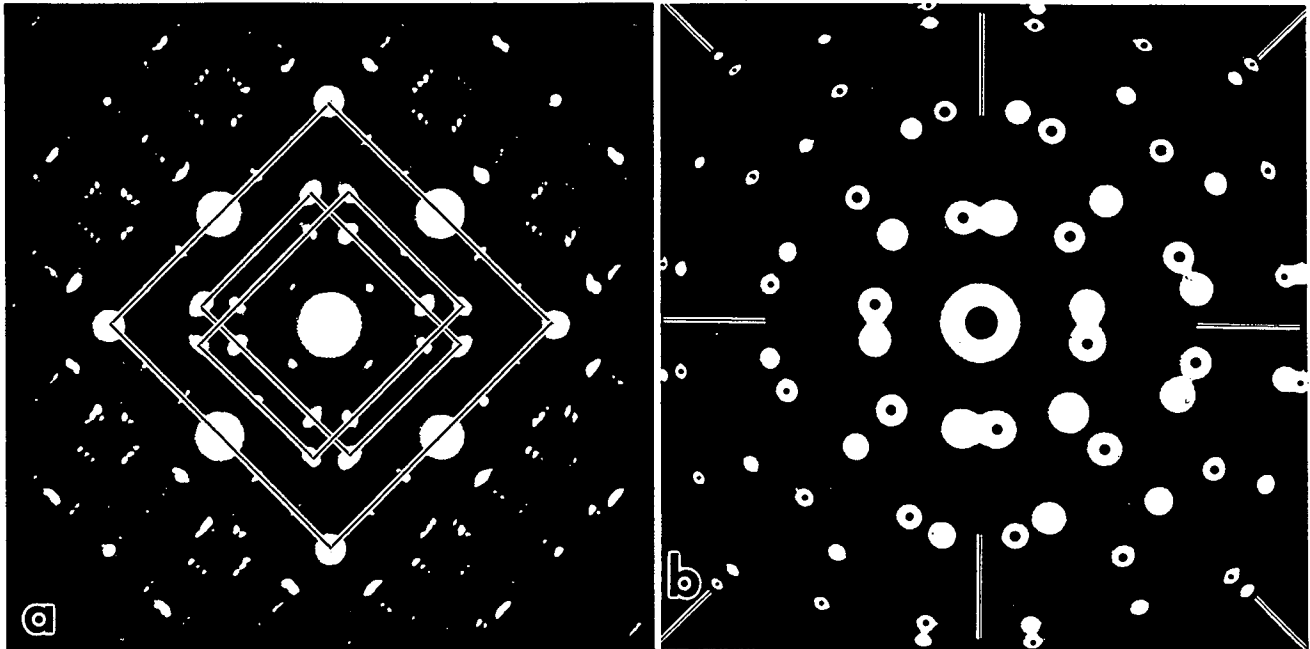


Fig. 2 Selected area diffraction patterns showing the observed orientation relationships. The pattern in (a) was obtained from a region of overlapping Al film and Si substrate. The square  $\langle 001 \rangle$  Si substrate and two rectangular  $\langle 110 \rangle$  Al patterns are outlined. The pattern in (b) is from an area of freestanding Al film and shows the two  $90^\circ$  rotated crystal orientations. For clarity, one of the two patterns has been marked with black dots. Mirror plane traces are indicated by white lines.

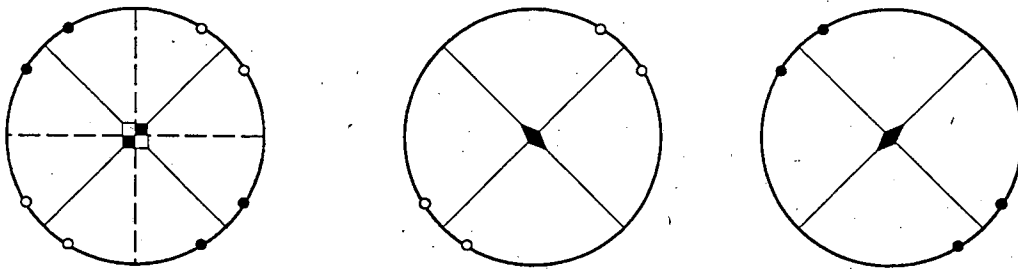


Fig. 3 Stereographic representation of the two-dimensional point group  $4mm$  as the combination of two groups of different color (orientation), each with  $2mm$  two-dimensional symmetry. Black-and-white symbols, broken lines and underlining indicate color symmetries. This schematic may be thought of as a graphic representation of equ. 1. The group  $2mm$  leaves both colors simultaneously unchanged while the set  $4^1(2mm)$  exchanges the two colors.

Under the same experimental conditions, deposition on a (111) substrate results in a tricrystal structure. Selected area diffraction patterns obtained from a region containing both Al and Si are shown in fig. 4a where the spots outlined by a hexagon are from the Si (111) substrate and the spots marked by squares originate from the Al. The Si (111) diffraction pattern is clearly evident from the hexagonal arrangement of spots whereas the Al diffraction patterns are obscured by double diffraction. The Al has three  $\{100\}$  orientation variants rotated by  $120^\circ$  forming a unique tricrystal arrangement as shown by square arrangement of spots in fig. 4a. The orientation relationship at the Al-Si interface is described as follows:



$$100_{\text{Al}} \parallel 111_{\text{Si}} - (\text{interface plane})$$

$$01\bar{1}_{\text{Al}} \parallel 01\bar{1}_{\text{Si}}$$

$$011_{\text{Al}} \parallel \bar{2}11_{\text{Si}}$$

The tricrystal Al diffraction pattern is more apparent when the Si is removed by back-thinning as shown in fig. 4b. Here the symmetry of the tricrystal structure is illustrated by indicating mirror planes of the composite diffraction pattern of the three grain orientations. Three types of symmetry elements can be identified from the tricrystal diffraction pattern: color, non-color and mixed elements. The color operations (underlined symbols) cyclically exchange the three individual patterns, the non-color operations (plain symbols) leave all three patterns simultaneously invariant and the mixed operations (bold symbols) exchange two of the patterns while leaving the third unchanged [8]. The two-dimensional tricrystal symmetry is of the non-crystallographic dodecagonal type  $\underline{12}mm$ .

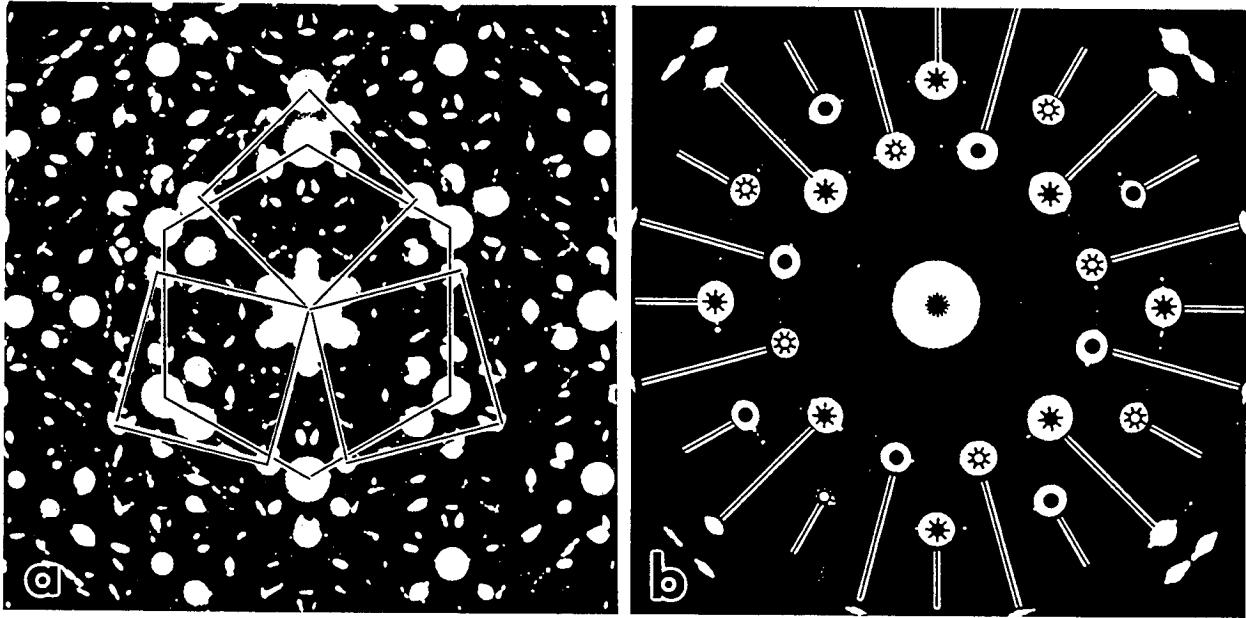


Fig. 4 Selected area diffraction patterns obtained from the Al tricrystal films and Si (111) substrate. In (a) the Si (111) substrate pattern is outlined by a hexagon and the three orientation variants of Al (100) are shown as squares. (b) the diffraction pattern obtained from the freestanding Al shows the point group symmetry of the tricrystal. The three individual patterns are identified by different symbols and the black lines represent twelve mirror planes in the tricrystal.

This three-color group can be described by the left coset decomposition

$$\underline{12}mm = \{4mm\} \cup \underline{3}^1\{4mm\} \cup \underline{3}^2\{4mm\}, \quad (2)$$

where the three cosets can be associated with the three colors or orientations. The first coset is the set of all operations that leave crystal 1 unchanged, while the second and third cosets are the set of all symmetry operations that change crystal 1 to crystals 2 or 3, respectively. Note that  $\{4mm\}$  is the group that leaves crystal 1 unchanged, but it may or may not exchange crystals 2 and 3, i.e. it has both gray and mixed elements. The two-dimensional point group corresponding to this three-color decomposition is shown in figure 5.

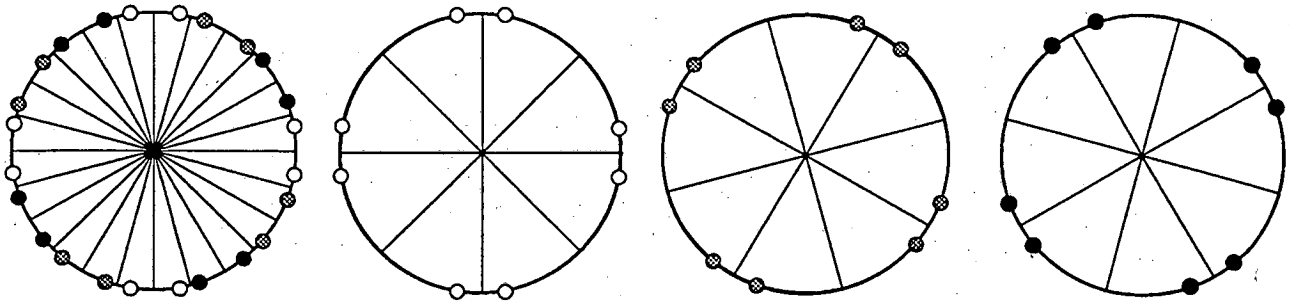


Figure 5: Stereographic representation of the two-dimensional point group  $12mm$  as the combination of three groups of different color (orientation), each with square  $4mm$  two-dimensional symmetry. This schematic may be thought of as a graphic representation of equ. 2.

The alternative decomposition

$$12mm = \{4\} \cup \{3^1, 3^2\} \{4\} \cup m\{12\} \{4\} \quad (3)$$

separates the three types of symmetry elements, gray, color-exchange, and mixed. The group  $\{4\}$  leaves all three colors simultaneously unchanged, the set  $\{3^1, 3^2\} \{4\}$  leads to cyclic exchange, and the set  $m\{12\} \{4\}$  (where  $m$  is any one of the 12 mirrors) leaves one color invariant while exchanging the other two. This decomposition is shown schematically in figure 6.

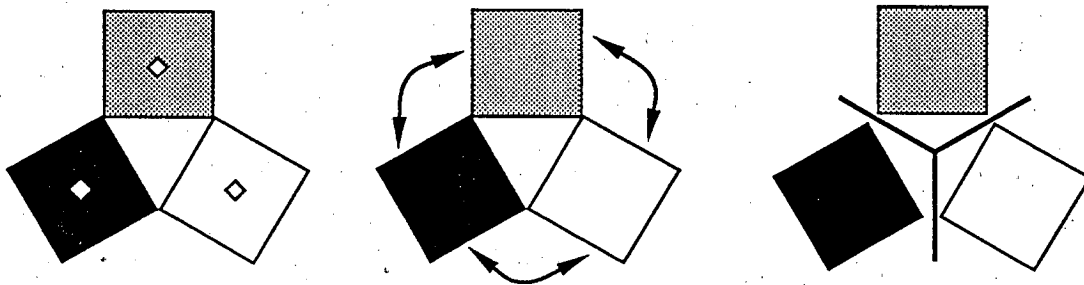


Figure 6: Symbolic representation of the three different types of symmetry elements of the tricrystal as shown in equ. 3, identity, cyclic exchange and mixed (mirror) operations.

It has been pointed out that the morphology of a crystal must contain the symmetry of its point group [6,7,9]. In the present case, the symmetry of the bicrystal grain boundary morphology must display  $4mm$  or higher two-dimensional symmetry and the morphology of the tricrystal must have dodecagonal  $12mm$  or higher two-dimensional symmetry. This means that in the bicrystal for every general grain boundary 8 equivalent boundaries can be found with the same structure and energy but with different orientation and for the tricrystal this multiplicity is 24. Boundaries that lie on mirror planes of the bi- or tricrystal are crystallographically degenerate and hence they represent symmetry-dictated extrema in structure and properties [6]. Such boundaries are therefore minima or maxima in energy. Close examination of the types of facet that develop upon annealing of these microstructures shows that multicrystal mirror planes are indeed preferred boundary inclinations.

In the bicrystal, two types of special facet are found; symmetrical boundaries that lie on a color exchange mirror and asymmetrical boundaries that lie on the (gray) mirror planes, i.e. the  $(100) \parallel (110)$

planes that are parallel in the two adjacent grains. An example of the first type is shown in the high resolution micrograph in figure 7. Note that this boundary is periodic and deviates slightly from the prescribed  $90^\circ$  angle of misorientation. It is in fact a  $\Sigma 99 \{557\} 89.4^\circ \langle 110 \rangle$  tilt boundary, at a misorientation of  $0.6^\circ$  less than that given by the substrate symmetry. This boundary has been investigated in some detail, and the observed structure was shown to be in good agreement with atomistic simulations which showed this particular structure and rigid body shift to be one of minimum energy [10]. The complementary symmetrical boundary for this misorientation of  $89.4^\circ$ , the  $\{7\ 7\ 10\}$  facet was never observed. This is not surprising since this interface has a much larger repeat period than the  $\{557\}$  facet.

The other preferred facet in the bicrystal structure were the asymmetrical boundary shown in a high resolution image in figure 8. This facet is parallel to one of the gray mirror planes of the bicrystal. At the boundary a  $\{100\}$  plane of one crystal meets a  $\{110\}$  plane of the other crystal. Hence this facet is parallel to low-index, widely spaced planes in both grains and is thus likely to be of low energy [11]. Notice that because of the direct juxtaposition of  $\{100\}$  and  $\{110\}$  planes the misorientation must be exactly  $90^\circ$  and hence there must be a defect accommodating the  $0.6^\circ$  deviation in misorientation where

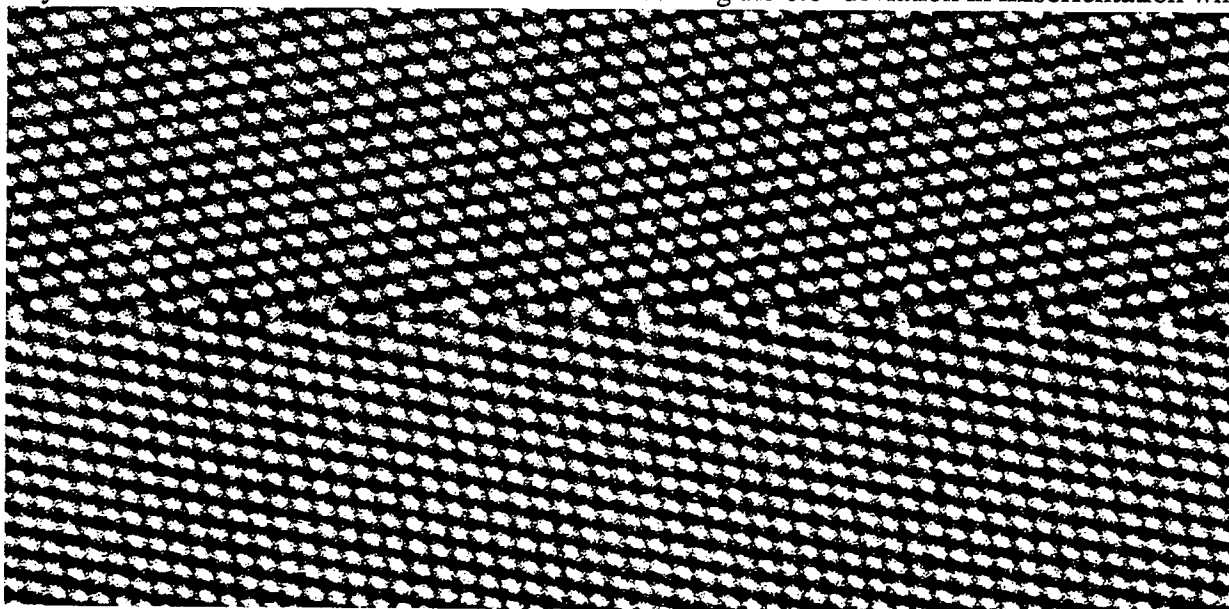


Figure 7: The most common facet of the mazed bicrystal structure, a  $\Sigma 99 \{557\} 89.4^\circ \langle 110 \rangle$  symmetrical tilt boundary, showing periodicity and highly localized relaxation.

the two preferred types of facet meet. Another result of this geometry is that this boundary must be quasiperiodic in structure because the lattice planes meeting across the boundary have spacings in the ratio of  $1:\sqrt{2}$ . Figure 8 shows that relaxation into structural units clearly occurs (see arrows). Although the spacing between structural units cannot be periodic, any local structural environment will be repeated elsewhere in a sufficiently long segment of boundary [12].

Facets in the tricrystal structure were also found to prefer multicrystal mirror planes. As pointed out above, all mirror operations of the tricrystal are mixed symmetry operations, i.e. they exchange two grain orientations while leaving the third invariant. If a boundary between two grains lies on a mirror plane of the third grain then it is a symmetrical boundary. If the boundary lies on a mirror plane of one of the two adjacent grains it is an asymmetrical boundary. A high resolution image of a symmetrical boundary facet is shown in figure 9. Notice how this is equivalent to the symmetrical boundary of the bicrystal shown in figure 7. Here, the prescribed misorientation is  $120^\circ$ . However, because of the 4-fold symmetry of the crystals along the common  $\langle 100 \rangle$  tilt axis this is identical to a  $30^\circ$  misorientation.

The boundary is again symmetrical and periodic with the periodicity of a  $\Sigma 65$  (740)(470)  $30.5^\circ$  [001] tilt boundary. Another symmetrical boundary segment observed was the  $\Sigma 53$   $31.9^\circ$  (720)(7 $\bar{2}$ 0) [001] tilt boundary [1]. As in the case of the bicrystal, the misorientation of these symmetrical segments is therefore not precisely that prescribed by the substrate but deviates sufficiently to allow periodic symmetrical facets to form. The repeat periods of these boundaries are larger than that of the symmetrical facet observed in the bicrystal.

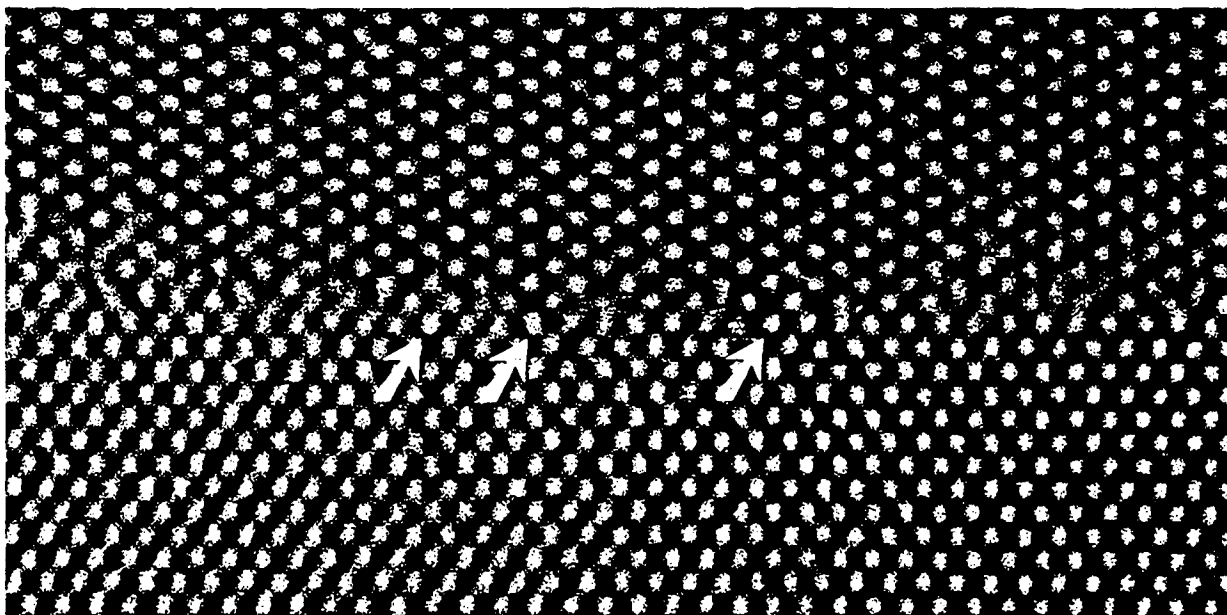


Figure 8: The other common facet of the mazed bicrystal structure, a  $90^\circ$  asymmetrical tilt boundary, showing absence of periodicity and highly localized relaxation (arrows).

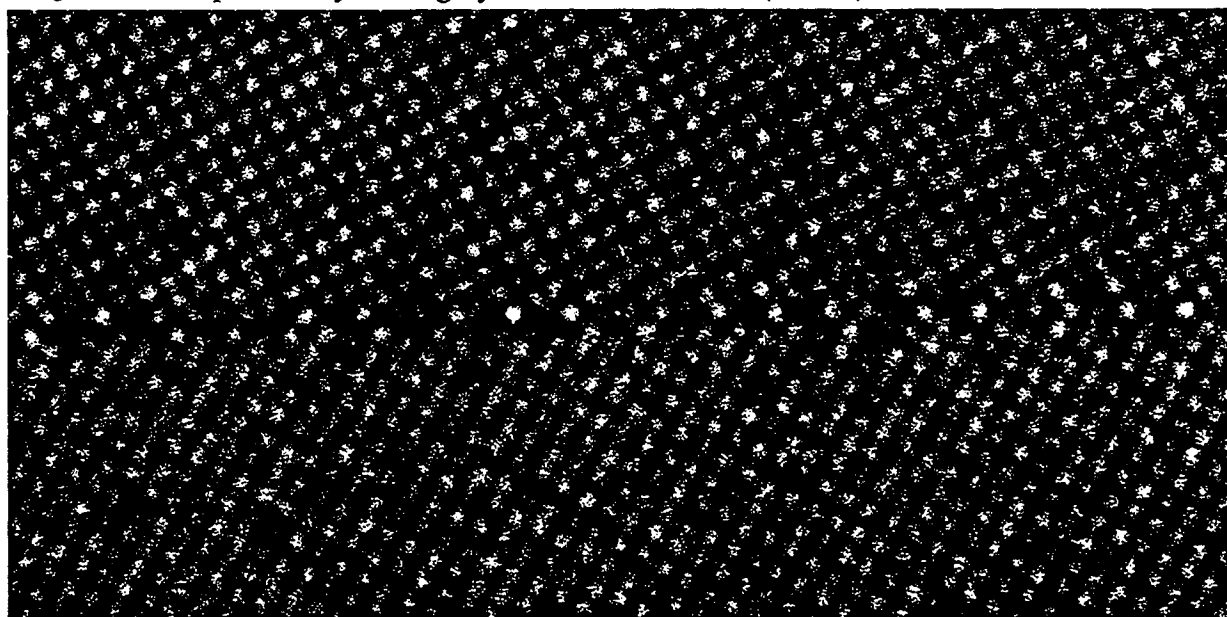


Figure 9: A symmetrical boundary facet in the mazed tricrystal structure, a  $\Sigma 65$  (740)(470)  $30.5^\circ$  [001] tilt boundary with relatively large repeat period.

Other boundary segments are found to lie along low-index mirror planes of one of the adjacent crystals, again similar to the case of the bicrystal where the asymmetrical boundary lies along two parallel low-index planes. However, not all boundaries are of pure tilt type. For the  $\langle 100 \rangle$  tilt axis of

the tricrystal structure, twist components, formed by boundaries that are not perpendicular to the surface are more common than for the  $\langle 110 \rangle$  tilt axis in the bicrystal.

It is interesting to examine the structure and morphology of triple junctions formed in the tricrystal microstructure. As mentioned before, for an ideal tricrystal structure all grain boundaries are of the same  $30^\circ \langle 100 \rangle$  tilt type. Thus, triple junctions will be made of three *identical* grain boundaries if the three boundaries meet at an angle of  $120^\circ$ . Figure 10 shows two special triple junctions of high symmetry, in which the boundaries lie on the  $\{100\}$  or  $\{110\}$  planes of the opposite crystal, respectively. Most triple junctions were not as symmetrical as those shown in figure 10. However, even with asymmetrical junctions it was found, that the adjoining facets tended to lie on one of the 12 mirror planes of the structure, leading to a distribution of inclinations that was peaked at  $15^\circ$  intervals. Quantitative evaluation of faceting behavior of both bi- and tricrystal morphologies is currently underway.

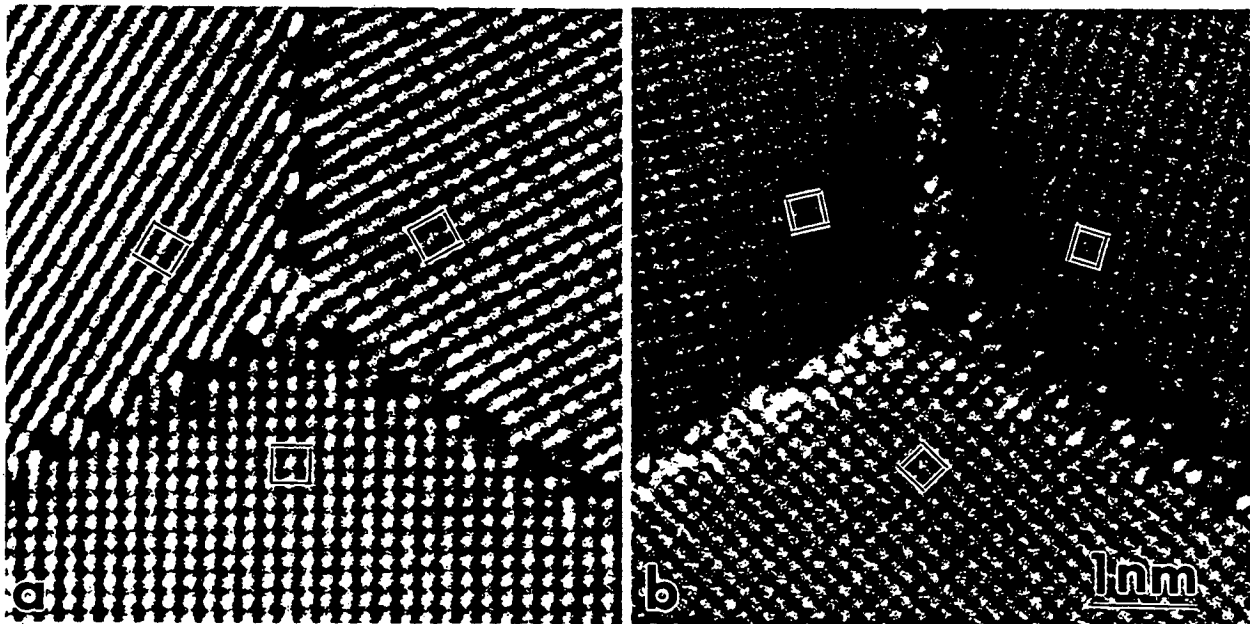


Figure 10: The two most symmetrical triple junctions in the tricrystal structure made up of symmetrical grain boundaries lying on the mirror planes of the opposite crystal, (a) for  $\{100\}$  mirror planes, (b) for  $\{110\}$  mirror planes. If no deviation from the precise  $30^\circ$  misorientation occurs, all three boundaries meeting at  $120^\circ$  in any triple line are identical.

## SUMMARY AND DISCUSSION

A similar investigation of faceting of grain boundaries in a range of  $\langle 100 \rangle$  and  $\langle 110 \rangle$  tilt boundaries in Au was reported by Goodhew et al. [13,14]. These bicrystals were made by a diffusion bonding technique in which two thin films of  $\langle 100 \rangle$  or  $\langle 110 \rangle$  orientation were twisted by the chosen angle of misorientation and subsequently welded together. During annealing of the bilayer films the twist boundary parallel to the free surfaces was unstable and migrated to become perpendicular to the film surface. This produced island grains of given misorientation surrounded by pure tilt boundaries. The faceting behavior was found to be more pronounced for the  $\langle 110 \rangle$  than for the  $\langle 100 \rangle$  tilt axis. In both cases preferred facets tended to lie on the  $\{100\}$  and  $\{110\}$  mean boundary planes, i.e. they tended to be symmetrical boundaries, or lie along  $\{100\}$  or  $\{110\}$  low-index planes of one of the two grains. These observations are identical to the findings of the work reported here for Al, both in the bi- and tricrystal films.

The present work has illustrated the color symmetry properties of multicrystal films formed by heteroepitaxial deposition on single crystal substrates. The bicrystal films were found to exhibit 4mm plane symmetry, one of the magnetic point groups while the tricrystal had a more complex three-color plane symmetry  $\overline{12}mm$  with a new type of symmetry element, a mirror that exchanges two colors while leaving the third color invariant. It was shown that such microstructures can be considered polycrystalline films with only two or three allowed grain orientations and only one type of grain boundary, i.e. boundaries with fixed misorientation but random inclination. In the bicrystal this misorientation was 90° around a common  $\langle 110 \rangle$  axis and in the tricrystal it was 30° around  $\langle 100 \rangle$ . Because interfaces tend to shorten by migrating into a position perpendicular to the film surface, all boundaries tended to be of pure tilt type. This was more strictly observed for  $\langle 110 \rangle$  tilt axis of the bicrystal than for the  $\langle 100 \rangle$  tilt axis of the tricrystal structure. Because of the anisotropy of grain boundary energy, certain inclinations were found as preferred straight facets. Fully annealed microstructures were well-faceted and the preferred boundary inclinations corresponded to a mirror symmetry plane of the bi- or tricrystal structure. The structure of such preferred facets was investigated by high resolution electron microscopy. In both bi- and tricrystal films it was found that small deviations (up to about 2°) from the prescribed misorientation occurred to allow nearby low-energy boundary facets to form.

Both microstructures are unique in several respects; in the bicrystal geometry, because only two grain orientations are allowed, there is only one kind of boundary with no triple junctions, and hence faceting is less constrained than in general polycrystalline materials. In the tricrystal structure there is also only one kind of boundary, but because there are three grain orientations, both dual facet junctions as well as triple junctions are now allowed. The  $\overline{12}mm$  gray symmetry of the tricrystal is a fairly close approximation the fiber texture typical for thin film growth and may thus serve as a model for studying mechanical and diffusional behavior of such films with pre-determined boundary structure.

Further multicrystal structures could be synthesized. The simplest possibility for a four-crystal structure arises from quadruple positioning in the growth of (111) Au on cleaved (100) NaCl. In this case there are four allowed grain orientations and two types of boundary, one of which is of the  $\Sigma 3$  type and therefore of much lower energy and much more strongly faceted than the other. Such a four-crystal structure has been reported by a number of authors and is under current investigation [15,16].

## REFERENCES

1. Thangaraj, N. and Dahmen, U.: MRS Proc. 238, 171 (1992)
2. Dahmen, U. and Westmacott, K.H.: MRS 229, 167 (1991)
3. Dahmen, U. and Westmacott, K.H.: Scr. Met. 22, 1673 (1988)
4. Madden, M.C.: Appl. Phys. Lett. 55, 1077 (1989)
5. Thangaraj, N., Westmacott, K.H. and Dahmen, U.: Appl. Phys. Lett., in press
6. Cahn, J.W. and Kalonji, G.: Proc. Conf. Solid-Solid Phase Trans., (1981), eds. H.I. Aaronson et al., p.3
7. Portier, R. and Gratias, D.: J. Phys. Coll. 43, C4-17 (1982)
8. Senechal, M.: Comput. Math. Applic, 16, 545 (1988)
9. Kalonji, G. and Cahn, J.W.: J. de Physique, Coll. 43, C6-25 (1982)
10. Dahmen, U., Hetherington, C.J.D., O'Keefe, M.A., Westmacott, K.H., Mills, M.J., Daw, M.S. and Vitek, V.: Phil. Mag. Lett., 62, 327 (1990)
11. Wolf, D. and Phillpot, S.: Mat. Sci. and Eng. A107, 3 (1989)
12. Sutton, A.P.: Acta Met. 36, 1291 (1988)
13. Allen, R.M. and Goodhew, P.J.: Acta Met. 25 1095 (1977)
14. Goodhew, P.J., Tan, T.Y. and Balluffi, R. W.: Acta Met. 26, 557 (1978)
15. Cosandey, F.: private communication
16. Tan, E.K. and Dregia, S.: EMSA Proc. 49, 558 (1991)

LAWRENCE BERKELEY LABORATORY  
UNIVERSITY OF CALIFORNIA  
TECHNICAL INFORMATION DEPARTMENT  
BERKELEY, CALIFORNIA 94720